Original

Crit Care & Shock (2009) 12:67-84

Differential Effects of Ventricular Pacing Sites of Contraction Synchrony and Global Cardiac Performance

Mohammed Alhammouri, Hyung Kook Kim, Yasser Mokhtar, Maxime Cannesson, Masaki Tanabe, John Gorcsan III, David Schwartzman, Michael R. Pinsky

Abstract

***Background*: Quantification of left ventricular (LV) dyssynchrony allows for objective measures of resynchronization therapy (CRT) effectiveness. We tested the hypothesis that site of LV pacing, fusion beats and baseline contractility alter contraction synchrony as quantified by regional and global measures of LV performance.**

***Methods and Results*: In 8 open-chested pentobarbital-anesthetized canine preparations we compared the effects of right atrial (RA), RA-high right ventricular (RV) free wall, as a model of left bundle branch block contraction pattern, RA-LV apex (LVa), RA-LV free wall (LVfw), and RA-RV-apical LV (CRTa) and RA-RV-free wall LV (CRTfw), as CRT. LV pressure-volume loops recorded using high-fidelity pressure and conductance catheters and echocardiographic angle-corrected color-coded strain imaging of mid-LV short axis views analyzed radial strain from six segments. To control for contractile state esmolol-induced beta blockage was studied, and in 5 dogs to control for RA and ventricular pacing fusion beat artifacts, repeat studies were done following AV node ablation. RA-RV pacing reduced stroke work (SW) (57±18 to 33±13* mmHg·mL,*p<0.05 vs RA pacing), decreased LV end-diastolic volume and induced marked radial dyssynchrony (maximal time difference between peak segmental strain) from 31±15 to 234±60* ms. Changes in radial dyssynchrony correlated significantly with changes in SW (r=-0.53, p<0.01). Dyssynchrony improved with both CRTa and CRTfw (69*±31 and 98*±63 ms, respectively) while SW only improved with CRTa (62±22* and 37±13 mmHg·mL, respectively * p<0.05 vs RV pacing). CRTa also tended to increased LV end-diastolic volume over RA-RV. Esmolol slowed HR from 118±10 to 108±10 beats/min* and tended to decrease contractility (end-systolic elastance (Ees) from 12.1±7.9 to 8.9±3.9 mmHg/ml, p=0.167) but did not alter the degree of RV-pacing induced dyssynchrony. AV ablation had no effect on the observed apical and free wall contraction differences seen during baseline conditions.**

***Conclusion*: Although both CRTa and CRTfw reduced contraction dyssynchrony, CRTa tended to improve global LV performance more by increasing end-diastolic volume. Thus, CRT may improve global LV performance differently, depending on the LV pacing site.**

Key words: Cardiac resynchronization therapy, canine model, esmolol, heart failure

From Cardiopulmonary Research Laboratory, University of Pittsburgh, Pittsburgh, PA (Mohammed Alhammouri, Hyung Kook Kim, Yasser Mokhtar, Maxime Cannesson, Masaki Tanabe, John Gorcsan III, David Schwartzman, and Michael R. Pinsky)

Address for correspondence:

Michael R. Pinsky, MD

606 Scaife Hall

3550 Terrace Street, Pittsburgh, PA 15261

Tel: 412-647-3587

Fax: 412-647-8060

Email: pinskymr@upmc.edu

Introduction

Cardiac resynchronization therapy (CRT) is an important treatment for the management of patients with heart failure and contractile dyssynchrony. (1,2) CRT reduces left ventricular (LV) dyssynchrony, improves global LV function and also improves long-term quality and quantity of life in some but not all patients with impaired contractile function. (3) CRT tends to improve LV systolic function in those patients with septal to LV free wall dyssynchrony, suggesting that the benefit of CRT results from reversing contraction dyssynchrony. (4,5) However, one recent clinical study documented that most of the immediate improved LV performance was related to improved LV diastolic compliance, rather than decreased LV end-systolic volume, (6) thus the mechanisms by which CRT improves LV performance are not clear. Furthermore, LV failure appears to exacerbate the effects of dyssynchrony on LV performance.

We recently described a novel angle-corrected subendocardial strain imaging approach to quantify radial mechanical dyssynchrony using an animal model of left bundle branch block (LBBB) and biventricular pacing and that radial strain dyssynchrony is associated with LV contractile impairment, as assessed by LV stroke work (SW) from pressure-volume analysis. (7) Using this approach we subsequently showed that such radial strain analysis quantified most, but not all of the global LV performance changes seen with pacing-induced dyssynchrony and CRT. (8) However, the effects of LV pacing site on LV performance pressure-volume relations, the impact of baseline contractile state on CRT effectiveness and the role of fusion beats in the subsequent CRT beats were not defined. Accordingly, we sought to quantify regional dyssynchrony as radial strain and phase angle discordance and correlated these changes with simultaneously measured LV pressure-volume relations by exploring the impact of LV free wall and apical pacing under baseline and esmolol infusion-induced beta adrenergic blockade. To control for pacing site artifact studies of isolated LV pacing were performed and to control for arterio-ventricular fusion beats studies were also performed following AV nodal ablation. To assess the potential role that ventricular interdependence might play in the observed changes in regional dyssynchrony and global LV performance, we also assessed the immediate impact of selective RV volume decrease, induced by IVC occlusion on LV diastolic compliance. Finally, in two dogs to control for ventricular interdependence, studies were performed with both an intact and open pericardium. In all other dogs studies were performed with an intact pericardium, whereas all studies were performed during open chest conditions.

Methods

Preparation: Eight mongrel dogs, weighing 19.6±1.4 kg were studied. The protocol was approved by the Institutional Animal Care and Use Committee and conformed to the position of the American Physiological Society on research animal use. All dogs were anesthetized with sodium pentobarbital (30 mg/kg induction; 1.0 mg/kg/h with intermittent boluses, as needed), their tracheas intubated (8 Fr. Portex endotracheal tube) and mechanically ventilated (Harvard dual-phase animal ventilator) with a 10 ml/kg tidal volume and frequency adjusted to maintain an arterial PCO_2 between 35-40 mmHg. A 6 Fr. 11 pole multi-electrode conductance catheter (Webster Laboratories, Irvine, CA) and an LV micromanometer catheter (MPC-500 Millar, Houston, TX) were placed for LV pressure-volume analysis via the right internal carotid artery and the left common carotid artery, as previously described by us. (9) These devices allowed for the continuous measure of LV pressure and volume allowing calculation of LV stroke volume (SV). The initial measures of LV end-diastolic volume and pressure were used to define baseline values for subsequent open-chest conditions. After a median sternotomy, a snare occluder was placed around the inferior vena cava (IVC) to transiently alter preload, allowing calculation of the end-systolic pressure volume relation needed to estimate end-systolic elastance (E_{es}) and preload recruitable stroke work (PRSW). The pericardium was opened and epicardial pacemaker leads were placed on the right atrium (RA), right ventricular (RV) free wall near the infundibulum, LV mid-free wall near the mid posterior-lateral wall, and LV apex for multi-site stimulation. The pericardium was re-opposed with multiple interrupted sutures and positive end-expiratory pressure (PEEP) applied to re-expand the lungs. Afterward, 5 cmH_2O PEEP was applied to maintain end-expiratory lung volume for the remainder of the experiment. Fluid resuscitation was performed prior to starting the protocol to

restore apneic LV end-diastolic volume to values similar to where they were prior to sternotomy.

Global hemodynamic data analysis: LV pressure, volume and electrocardiogram (ECG) signals were digitized at 150 Hz and stored on disk for off-line analysis. The following hemodynamic parameters were assessed for LV contractile performance: LV end-systolic pressure, peak positive dP/dt (+dP/dt max), peak negative dP/dt (-dP/dt max), the time constant for active LV pressure decay (tau), SV, and stroke work (SW) using standard formulae. (6) The slope of the end-systolic pressure-volume relationship (ESPVR), or E_{es} and PRSW, the relation between SW and LV end-diastolic volume were calculated as relatively load independent measure of contractility. E_{es} was defined as the slope of maximum pressure/volume points from each LV loop during IVC occlusions using an automated iterative linear regression technique as previously described by us in this preparation. (9) We also estimated the impact of BiV pacing on diastolic interdependence by the method of Bleasdale et al (6) wherein the immediate decrease in LV end-diastolic pressure prior to a change in end-diastolic volume during a rapid IVC occlusion, was taken to reflect the impact of right ventricular (RV) decompression on LV filling.

Echocardiography and strain imaging: An echocardiographic system with tissue Doppler (TD) capabilities was used (Aplio SSA-770A, Toshiba Medical Systems Corporation, Tokyo, Japan) with a 3.0MHz transducer. Digitized routine and color-coded TD images were acquired from mid-LV short-axis levels using epicardial imaging and a transducer stand. TD system frame rates were a minimum of 49 frames/sec with a pulse repetition frequency of 4.5 kHz. Velocity ranges were from ±17.0 cm/sec to ±13.0 cm/sec to select the lowest possible range to maximize the sensitivity of low velocity values while aliasing did not occur. Color TD video data set were analyzed off-line using custom software as described elsewhere in detail (10-13) (ApliQ, Toshiba Medical Systems Corporation, Tokyo, Japan). Briefly, the myocardial vector (V) of motion toward a manually placed point of contraction center was calculated as: V motion=V beam/cosine θ, where θ is the angle of incidence of the ultrasound beam. Sectors were masked where the angle of incidence approached 90º and Doppler calculations are not possible. Strain was calculated as time integral of velocity gradient that was calculated along radii of a distance (Δr) toward the contractile center. Angle corrected, color-coded Lagrangian strain was calculated as % wall thickening toward the contraction center and displayed on a continuous scale from dark red to bright orange-yellow as positive strain corresponding to wall thickening. Regions of interest were manually drawn on six segments of the mid-LV short axis view (mid-septum, antero-septum, antero-lateral, postero-lateral, posterior and inferior) as linear polygons placed in the inner third of the wall. This subendocardial region was selected to represent the major component of transmural thickening and to minimize translational or right ventricular effects on regional LV wall dynamics. A tracking algorithm was employed with manual adjustment of the size and shape of the regions of interest to maintain its subendocardial location throughout the cardiac cycle.

Regional contraction synchrony analysis: Time-strain curves were constructed from color-coded strain data as previously described by us in this preparation. (7) Time-to-peak subendocardial strain was determined from the onset of the QRS complex in all 6 segments. Dyssynchrony index was defined as the maximum difference in time from earliest to latest segment among 6 segments, and standard deviation of time-to-peak strain from all 6 segments was also calculated. To assess overall radial systolic function, an overall time-strain curve was also reconstructed by averaging 6 segmental time-strain curves. Inter- and intra-observer variability were 4.7±3.7% and 4.1±5.2% for time-to-peak strain, and 7.8±6.3% and 6.2±5.2% for global strain.

Protocol: All the above measurements were made with respirations suspended at end-expiration at 5 cmH_2O PEEP to control for the effects of cardiopulmonary interactions. The protocol consisted of first creating a stable apneic steady state, then noting the effect of a transient IVC occlusion and release on the measured variables. Pacing steps in the study were as follows: To avoid retrograde AV conduction for all pacing steps of the protocol RA pacing was performed at frequencies 5-10/min above the intrinsic rhythm ventricular pacing. To control for any heart rate-specific changes in global and regional function RA pacing was compared to

apneic sinus rhythm. All subsequent ventricular pacing studies were then done with simultaneous RA pacing. To induce a LBBB contraction pattern high RV free wall pacing was used. We then compared the impact of counter-pacing at two different LV sites on the RV-pacing induced LBBB contraction pattern, referred to as apical CRT (CRTa) and free wall CRT (CRTfw). We chose to pace at the apex and posterior-lateral LV free wall at the mid ventricular level below the left circumflex artery. To control for LV pacing-specific changes in contractile performance independent of an intrinsic LBBB contraction pattern, we also studied the effect of isolated LV apical (LVa) and free wall (LVfw) pacing. The order of apical and free wall pacing was alternated among sequential animals to eliminate any sequencing effects. Pacing was sustained for >30 seconds before measurements were made for each step so that hemodynamic equilibrium could be established. In practice, hemodynamic stability usually took <15 seconds to occur. Between each ventricular paced rhythm interval, the animals were returned to RA pacing and all hemodynamic variables allowed returned to baseline levels before the next step in the protocol was started. This series of pacing runs is referred to as control conditions and can be summarized as: RA, RA-RV, RA, RA-LVa, RA, CRTa, RA, RA-LVfw, RA, CRTfw (with the order of apical and free wall alternating between animals).

In several of the animals at the end of the above pacing sequence, we also studied the immediate effects of varying the sequencing the pacing from RA alone to RV and then either apical BiV or free wall BiV as a step-wise two to three beat each progression. These rapid sequence pacing sequences were done to see the immediate effects of pacing sequence independent of global changes in autonomic tone that may occur under steady state pacing conditions. This rapid progression of pacing site is referred to as a "rainbow" and was done to document the mechanical effects of pacing site independent of the time-dependent reflex changes in vasomotor tone potentially induced by pacing-induced changes in global performance.

Following these initial pacing runs, we induced acute beta adrenergic blockade by infusion of high dose esmolol (bolus of 20-40 mg and infusion at 2 mg/min i.v.) to impair LV contractility. This condition is referred to as Esmolol. During Esmolol the above pacing protocol was repeated as above using the same pacing heart rate and sequence as during control conditions. Then following the AVF series, in the initial 5 animals studied we also examined the effect of pacing under conditions of complete AV blockade to control for the potential effect that simultaneous atrio-ventricular pacing my have in creating fusion beats. Access to the central circulation was gained via right femoral and internal jugular veins. Ablation (Biosense, Webster) and intracardiac echocardiography (ICE, Boston Scientific) catheters were advanced to the right atrial body. Using intracardiac echocardiography, the ablation electrode was maneuvered into contact with the compact AV node, taking care to avoid direct contact of ventricular myocardium. Unipolar (cutaneous ground) application of radiofrequency energy was delivered via this electrode using a commercial generator (Biosense Webster), with power titrated until onset of junctional rhythm and then AV block. We then repeat the above pacing sequence but without the RA alone steps. This series is referred to as AV blockade.

Statistical analysis: Data are expressed as mean±SD. Following statistical analysis we performed a 2-way analysis for repeated measures with a Bonferroni *post hoc* comparison. Statistical significance reports differences corresponding to a $p < 0.05$.

Results

Effect of pacing site on global LV function: The mean LV measured and calculated hemodynamic values for all 8 dogs during control and esmolol infusion and in the 5 dogs following AV nodal ablation are shown in **Table 1**. As reported by others tau was unaffected by pacing but decreased during esmolol infusion. Stable heart rates were achieved by RA pacing for reproducible baseline measurements. As expected, RA pacing created global hemodynamic conditions indistinguishable from sinus rhythm. Thus, RA pacing was taken to reflect native contraction but as a heart rate similar to all other pacing conditions. All subsequent comparisons are made between RA pacing and other pacing states.

RV pacing was associated with both increased dyssynchrony and reduced global cardiac performance. As compared to

RA, RV was associated with a decreased LV end-systolic pressure, SW and peak negative dP/dt. LV SV, PRSW and peak positive dP/dt also tended to decrease and tau tended to increase, but not significantly. The two sites for LV pacing during RV-induced dyssynchrony had different effects on global LV performance. CRTa increased LV end-systolic pressure, SV, SW and CO above RV pacing levels and also increased both LV SV and SW over CRTfw levels. Except for returning LV end-systolic pressure to RA levels, CRTfw did not alter global LV performance over RV levels. **Figure 1** illustrates the effect of pacing on the LV pressure-volume relationship under RA, RV and both CRTa and CRTfw conditions. Electronic supplemental **Figure 1** shows all individual animal steady state LV pressure-volume loops and their associated E_{es} relations. Since LV pacing alone alters LV contraction pattern and may influence the CRT pacing behavior we compared the effect of selective LV pacing without RV pacing-induced LBBB on LV contraction patterns using both apical LV and free wall pacing sites. Both LVa and LVfw resulted in LV performance similar to both RA and apical BiV. **Figure 2** illustrates the effects of selective LV pacing versus CRT pacing on LV pressure volume relationships for the same animal as shown in **Figure 2**. Note that the uni-site pacing LV pressure-volume loops are similar, but not identical, to those for their respective CRT conditions. Qualitatively similar findings were seen during Esmolol (**Table 1**).

Esmolol infusion rapidly induced a reduction in HR and peak positive LV dP/dt (118±10 to 108±10 beats/min, and 1987±396 to 1640±257, respectively, $p < 0.05$), increased tau (39.8±8.5 to 47.3±8.7 msec, $p < 0.05$) and also tended to reduce E_{es} but to a non-significant degree (12.1±7.9 to 8.9±3.9 mmHg/ml, $p = 0.167$). However, the impact of pacing on global LV performance during AVF was similar to that seen under baseline conditions.

Effect of pacing on regional strain time activity relations: The impact of pacing on radial strain parameters for a short axis six-segment sample is summarized in **Table 2** for all animals. As compared to RA, RA-RV increased both measures of dyssynchrony. Importantly, although both CRTa and CRTfw decreased both measures of dyssynchrony relative to RA-RV, these decreases resulted in dyssynchrony values still higher than RA pacing (**Figure 3**). Interestingly, although the LV pressure-volume loops for LVa and CRTa were similar (**Figure 2, Figure E1**), LVa had a higher dyssynchrony values than CRTa during baseline, but not during Esmolol. Changes in radial dyssynchrony correlated with changes in LV SW ($r = -0.53$, $p < 0.01$) (**Figure 4**). These data suggest that measures of dyssynchrony and global performance may quantify different aspects of LV function.

Effect of fusion beats on LV performance during pacing: To address the potential issue of fusion beats from simultaneous RA pacing in our model, we also studied five animals after AV nodal ablation. The LV pressure-volume relations and radial strain data for the pacing data from these five animals were indistinguishable to that observed prior to AV nodal ablation (**Tables 1** and **2**). Thus, it appears that our findings during non-A-V node ablation were not due to fusion beats arising from atrial activity.

Ventricular interdependence: We measured the ΔP induced by IVC occlusion during control and pacing using the method of Breasdale et al. (6) In no animals was ΔP >2 mmHg, suggesting that ventricular interdependence was not a primary determinant of the changes in LV end-diastolic volume during CRT in our model. Furthermore, in the two final animals in our study in which a pericardiotomy was performed, although absolute LV volumes increased, CRTa also increased LV EDV over RA-RV pacing, whereas CRTfw did not alter LV EDV. Furthermore, no ΔP was seen during IVC occlusion. An example for one of those animals is shown in **Figure 5**. In this example we also display the instantaneous mechanical effects of rapid pacing progression (rainbow) on global LV performance. As can be seen, the instantaneous effects of pacing site induce immediate changes similar to their steady state counterparts.

Discussion

Our results agree with previous investigators by reporting that the site of LV pacing determines the degree to which regional dyssynchrony and global LV function are improved. (5,14) The mechanisms by which global LV performance

improves are complex but do not appear to be influenced by esmolol-induced changes in contractility, fusion beats, and ventricular interdependence nor to be tracked by changes in E_{es}. While CRTfw improves LV developed pressure and LV SW for a constant end-diastolic volume and stroke volume, CRTa improves global systolic function by simultaneously increasing LV end-diastolic volume and stroke volume while decreasing LV end-systolic volume. These data agree with previous studies by others in similar canine models. For example, Peschar et al (15) also showed the LV apical pacing produced maximal LV performance, but they did not use a LBBB model. However, Bordachar et al (16) and Helm et al (17) demonstrated that apical LV site was superior to free wall LV site in CRT pacing in a heart failure model. Collectively these data support the concept that apical LV pacing may be better than free wall pacing if no conduction block exists because it optimizes contraction synchrony. The Helm et al study used MRI imaging to closely map lines of equal dyssynchrony from pacing. Though highly insightful and elegantly performed MRI is not applicable for routine analysis whereas echocardiography is. Thus, our data, though supporting the Helm et al findings extend this approach into bedside echocardiographic analyses. Interestingly, Frias et al (18) demonstrated in a model of A-V nodal blockade that E_{es} was altered by pacing if originating from the apical RV, apical LV or BiV regions, with apical LV pacing having the greatest E_{es}. However, our A-V nodal blockage data did not show any changes in E_{es} although apical BiV sustained its better stroke volume, SW and trend to a higher E_{es} value.

This animal study addressed many aspects of cardiac resynchronization. To model LBBB we used high RV free wall pacing, as previously described. (9,17) We then performed CRT using two different LV pacing sites, the apex and lateral free wall. Lateral wall pacing sites are often used in clinical studies of CRT. Unlike clinical trials where LV free wall pacing often appears to provide contractile benefit, (1) we consistently saw that apical pacing improved contraction synchrony better, as manifest by the lower dyssynchrony index and higher stroke work. Several other studies also reported that apical pacing improved contractile synchrony best, (17,19,20), although the LV apex is typically inaccessible for lead position by the epicardial coronary veins used clinically. Clearly, clinical studies use not only heart failure subjects, but those with a prolonged QRS interval associated with anatomically-induced LBBB. (3) To the extent that these two anatomical realities (structure change and conduction block) interface with the pacing-induced resynchronization, these differences may explain the better resynchronization performance observed with lateral wall LV pacing in some human studies, as compared to our animal study and those of others (19,20). In support of defining LV lead placement by the resultant change in dyssynchrony, Vanderheyden et al (21) noted that decreased dyssynchrony, as documented by echocardiography, was associated with optimal LV performance. Importantly, changes in LV maximal dP/dt were poor predictors of improvement and more direct measures of cardiac performance, like, LV SW, predicted better long-term results. (22) However, we sampled LV pressure at 150 Hz which may be too low to distinguish major changes in LV dP/dt. However, our data comparing apical to free wall CRT support these latter findings, in that global LV performance indicators showed different responses to pacing-induced dyssynchrony and CRT. Thus, measures of both dyssynchrony and global LV performance need to be combined when assessing the effectiveness of CRT.

High free wall RV-pacing induced a LBBB contraction pattern that decreased global LV performance and induced dyssynchrony, as can be quantified by tissue Doppler radial strain analysis and its associated dyssynchrony index. High RV outflow tract pacing has been used by others to model LBBB contraction patterns. (9,17) Furthermore, LBBB contraction patterns impair global LV performance. (23) CRT using either apical or free wall LV pacing to counterbalance this induced LBBB contraction pattern reduces regional radial dyssynchrony, but may not improve global LV function by the same degree. Furthermore, the effects of free wall versus apical LV pacing sites have markedly different effects on regional contractile strain patterns, independent of their isolated effects on LV contraction because regional radial strain activity among regions is differentially altered.

Finally, our findings of an increased LV end-diastolic volume during CRTa as compared to RA-RV pacing agrees with those observations reported by Bleasdale et al (6) in patients with congestive heart failure undergoing CRT. However, unlike their patients with both organic dyssynchrony and congestive heart failure, our animals with pacing induced dyssynchrony and normal myocardial structure displayed no obvious ventricular interdependence. Thus, the mechanism

for which LV EDV increases with CRTa in our model may not be similar to that proposed by Bleasdale in their human study. First, we saw minimal pericardial restraint using their ΔP analysis during IVC occlusion and the effect persisted following pericardiotomy. Second, the degree of LV dilation during CRTa was unaltered by esmolol infusion, suggesting that changes in global contractility do not influence these effects. This second argument may not be completely valid. In review of the experimental condition during these latter two studies during open pericardium conditions, it was clear that the echocardiographic probe was depressing the anterior surface of the heart. Thus, even though the heart dilated as compared to closed pericardium conditions, some interdependence could still have been maintained. Finally, one would presume that if RV dilation caused reduced LV diastolic compliance, by the process of ventricular interdependence, then this effect would be augmented by decreasing contractility with its associated need for fluid resuscitation to sustain blood flow. It did not and, thus, we think that the cause of increased LV end-diastolic volume during BiV apical pacing is probably not due to decreased ventricular interdependence.

An important potential cause for our observed increases in LV EDV during CRTa includes pacing-induced improved LV diastolic relaxation. Normal diastolic induces a suction-like effect augmenting LV filling. (24) Grover and Ganz (25) demonstrated that pacing-induced contraction dyssynchrony could decrease LV diastolic compliance. Since patients with LBBB and heart failure have greater diastolic dysfunction than do heart failure patients without LBBB (26) it is possible that if CRT minimizes this dyssynchrony, it would be associated with improved LV diastolic function. RV pacing-induced LBBB pattered contraction is associated with delayed septal re-polarization. Potentially, this could make the septum appear stiffer during diastole than would have been predicted from the associated RV volume. In essence, LBBB-like contraction patterns may create a pseudo-ventricular interdependence. If septal activation were synchronous with free wall contraction then all portions of the ventricle may relax synchronously improving LV diastolic compliance. Apical BiV pacing induces early septal excitation that might allow for a more complete septal relaxation as compared to either RV pacing or free wall LV pacing. Although this hypothesis would explain our lack of IVC occlusion reductions in LV pressure as seen by Bleasdale et al (6), it does not explain their findings of an immediate decrease in LV end-diastolic pressure without a change in end-diastolic volume. Those differences may relate to the fundamental difference between normal cardiac function in our animals and congestive heart failure conditions in their patients.

Finally, ventricular activation by epicardial pacing requires activation of the His-Purkinje system. (23) However, the penetration of the subendocardial His-Purkinje network onto the epicardial surface is heterogeneous. Apical epicardial penetration is common whereas lateral free wall penetration is variable. (27) Potentially, the improved LV function seen with CRTa over CRTfw reflects these epicardial His-Purkinje system regional differences that favor a more direct activation of the system form an apical site.

Limitations and implications of these data: Several specific aspects of these data are both consistent with prior studies and different from some clinical observations, and these differences may be relevant to the associated physiology. First, we used high outflow tract RV pacing as our model of LBBB contraction dyssynchrony as has been done previously (9,17) and simultaneous LV pacing to offset dyssynchronous contraction. Neither process exactly models clinical CRT. Right ventricular outflow tract pacing is not the same as intrinsic LBBB with its associated structural changes. However, the contraction pattern induced by RV pacing was identical to that seen in patients with LBBB. (23) Namely, we saw an early septal contraction followed by a later free wall contraction and septal relaxation, the sum of which profoundly reduced LV contraction synchrony. Furthermore, we paced the atria and ventricular simultaneously in this model. Thus, the normal atrio-ventricular coupling may have been disturbed and fusion beats may have induced un-physiologic contraction patterns. However, the dyssynchronous contraction patterns seen were unaltered following A-V nodal ablation suggesting that atrio-ventricular coupling is not a primary determinant of the observed hemodynamic responses. Finally, the timing of LV pacing during CRT was simultaneous with RA and RV pacing, whereas with clinical CRT timing of LV pacing is altered to maximize LV filling and SW. Potentially, the differences in dyssynchrony indexes and SW seen between CRTa and CTRfw might have been minimized by differently

timed atrial and LV pacing.

Second, we studied a previously healthy animal without evidence of structure cardiac abnormalities and during open chest conditions, albeit with an intact pericardium. And although we impaired cardiac contractility using esmolol to blunt β-adrenergic stimulation, the baseline structure of these hearts was normal. Furthermore, in keeping with a normal baseline myocardium, although esmolol infusion reduced heart rate and induced an increase in LV volumes, the decrease in both E_{es} and PRSW was not significant, and both cardiac output and mean arterial pressure were unaltered. Clearly esmolol-induced AVF does not induce the structural wall thinning and loss of adrenergic receptor response seen in chronic congestive heart failure. This fact may directly influence the lack of ventricular interdependence we saw when we opened the pericardium in two animals. Pericardiotomy should have markedly decreased any right to left ventricular interdependence effects during both diastole (28) and systole (29). It did not. This suggests that the observed LV dilation during apical BiV pacing reflected processes other than improved RV ejection.

Clinical implications: These basic animal studies have three implications for clinical trials. First, cardiac resynchronization therapies are aimed at reducing contractile dyssynchrony. However, the relation between careful measures of regional dyssynchrony and global LV performance in the acute setting may not be tightly linked. Second, the site were pacing needs to be done to minimize contraction dyssynchrony is dependent on the nature of the baseline dyssynchrony, such that targeting one specific region of the LV may not be as effective as identifying that region when pacing reducing dyssynchrony the most. Although we saw less dyssynchrony and better global LV performance with apical BiV, this site is usually not accessible with routine percutaneous coronary vein lead placement, though accessible through surgical epicardial lead placement. Finally, the goal of CRT may not be to maximize immediate mechanical performance more than reducing overall contractile dyssynchrony. Although not supported directly by these studies, the implication is that short-term LV performance benefit induced by CRT may not be sustained unless contractile dyssynchrony is also minimized. This final implication awaits further validation clinical studies but follows logically on the results of these animal data.

Acknowledgements:

This study was supported in part by NIH awards HL04503, HL067181 and HL073198.

The authors wish to thank Lisa Gordon and Don Severn for their excellent technical assistance.

Table 1. Hemodynamic Effects of Pacing Site on Global Left Ventricular Performance

Baseline Conditions (n=8)

Parameter	SR	RA	RV	Apical LV	Free wall LV	CRTa	CRTfw
HR, bpm	118±10*	127±8	127±8	127±8	127±8	127±8	127±8
EDV, mL	33.8±11.8	33.2±11.7	31.6±11.4*	37.3±14.0*	33.1±11.4	39.3±14.7*†	33.2±12.2‖
ESV, mL	27.3±10.1	27.1±9.9	26.4±10.6	28.7±11.3	27.7±10.5	31.1±12.3*†	28.1±11.4‖
SV, mL	6.4±2.8	6.1±2.5	5.2±1.7	8.6±3.4*	5.4±1.7	8.2±2.7*†	5.1±2.0‖
ESP, mmHg	104±13*	108±11	88±10*	96±6*	101±13	93±10*†	92±9*†§
EDP, mmHg	11±4	10±4	8±3*	8±4*	9±4	8±4*	8±4*
LV(+)dP/dt, mmHg/s	1987±396*	2163±461	1614±371*	1940±344*	1942±446	1836±371*†	1767±272*
LV(−)dP/dt, mmHg/s	−1621±369*	−1753±360	−1206±255*	−1437±219*	−1533±440	−1304±295*†‡	−1305±205*
SW, mmHg · mL	59±20	57±18	33±13*	68±23	47±14	62±22†	37±13*§‖
CO, mL/min	764±350	778±345	667±239	1095±461*	696±244	1061±378*†	656±281‖
E_{es}, mmHg/mL	12.1±7.9	10.7±3.7	13.7±6.8	13.7±8.1	10.8±8.2	14.4±4.0	15.3±6.0
PRSW, mmHg	11.6±7.6	7.1±3.7	8.1±4.9	7.2±11.6	9.5±6.1	12.4±8.8	10.0±7.7
E_{max}, mmHg/mL	31.2±26.1	23.5±11.3	29.6±26.8	27.8±21.9	25.4±24.8	27.5±22.2	28.8±13.6
Tau, msec	39.8±8.5	39.1± 6.2	39.6±8.3	40.4±9.0	43.9±11.3	41.4±10.7	42.9±9.8

During Esmolol Infusion (n=8)

Parameter	SR	RA	RARV	Apical LV	Free wall LV	CRTa	CRTfw
HR, bpm	108±10*#	119±12#	120±11#	120±10	120±10#	120±11#	120±10#
EDV, mL	37.3±13.6#	36.8±13.1#	34.2±13.1*#	38.8±14.0	35.1±13.2	39.0±13.8†	34.5±13.2*‖
ESV, mL	30.0±11.4#	29.8±10.8#	28.8±11.4#	31.2±12.0#	20.1±11.8#	31.5±12.2†	29.7±11.9†‖
SV, mL	7.2±4.1	6.9±3.4	5.4±2.8*	7.6±2.8*	4.9±2.4*	7.6±2.6†	4.8±2.4*‖
ESP, mmHg	102±13	105±13	83±13*	91±14*	90±13*#	87±14*	88±18*
EDP, mmHg	13±3*	11±3	8±3*	9±3*	9±3*	8±3*	9±4*
LV(+)dP/dt, mmHg/s	1640±257*#	1776±292#	1319±275*#	1471±261*#	1389±264*#	1410±253*†#	1338±323*#
LV(−)dP/dt, mmHg/s	−1503±252*#	−1587±286#	−1104±289*#	−1242±311*#	−1236±311*#	−1204±321*†	−1183±425*
SW, mmHg · mL	58±24*	58±19	31±15*	56±18	35±15*	54±14†	31±16*‖
CO, mL/min	784±437	817±392	657±373*	924±382	600±327*	922±360†	586±332*‖
E_{es}, mmHg/mL	8.9±3.9	9.4±4.2	10.8±4.8	12.6±6.2	9.6±2.9	11.5±6.4	13.2±6.3
PRSW, mmHg	6.8±4.4#	6.9±4.2	5.7±7.2	14.0±12.6	6.6±4.7	13.5±10.2†	5.1±4.5‖#
E_{max}, mmHg/mL	28.4±19.9	24.7±14.7	42.6±46.4	17.7±10.9	20.2±9.9	23.7±16.3	20.3±7.4
Tau, msec	47.3±8.7	45.0±7.4	46.6±11.0	48.6±11.9	50.1±11.3	45.4±12.5	48.0±12.4

Following A-V Node Ablation (n=5)

			Free wall		
Parameter	**RV**	**Apical LV**	**LV**	**CRTa**	**CRTfw**
HR, bpm	87±6#	87±5#	87±6#	87±5#	88±6#
EDV, mL	47.2±10.8#	52.1±12.9	47.5±11.1#	53.4±13.0†	47.4±12.1#
ESV, mL	38.7±8.9#	40.0±10.7	40.5±9.7#	42.5±11.5‡	40.3±10.1#
SV, mL	8.5±3.2#	12.1±2.8	7.0±2.2	10.9±2.3‡	7.4±3.1†#
ESP, mmHg	103±17	102±13	110±17	112±19†‡	114±17†§
EDP, mmHg	11±5#	10±4#	11±5#	11±5#	11±5#
LV(+)dP/dt, mmHg/s	1494±219	1602±191	1665±146	1864±239†	1737±186†
LV(−)dP/dt, mmHg/s	−1396±366	−1436±344	−1533±378	−1608±382†	−1632±402†§
SW, mmHg · mL	48±6#	94±35	51±8	98±26†	53±7
CO, mL/min	728±231	1047±207	606±156	944±166	636±232
E_{es}, mmHg/mL	10.6±6.8	7.5±1.5#	8.0±2.7	8.3±4.2	9.7±2.7
PRSW, mmHg	10.6±5.7	9.8±5.6	8.8±3.0	11.1±5.2	5.7±4.6
E_{max}, mmHg/mL	37.4±24.5	18.4±7.8	14.4±6.0	19.1±11.2	11.3±7.4
Tau, msec	46.0±18.6	46.1±18.7	48.7±19.4	43.8±16.7	44.9±17.8

Abbreviations: HR, heart rate; EDV, end-diastolic volume; ESV, end-systolic volume; SV, stroke volume; ESP, end-systolic pressure; EDP, end-systolic pressure, LV(+)dP/dt, maximum LV dP/dt during systole; LV(-)dP/dt, maximal negative dP/dt during diastole; SW, stroke work; CO, cardiac output; E_{es}, end-systolic elastance; PRSW, preload-recruitable stroke work, in mmHg/mL; E_{max}, maximal elastance. Pacing modes: SR, sinus rhythm, RA, right atrial pacing; RV, simultaneous RA and RV outflow tract pacing; apical LV, simultaneous RA and LV apex pacing; free wall LV, simultaneous RA and LV free wall pacing; CRTa, simultaneous RA, RV outflow tract and LV apex pacing; CRTfw, simultaneous RA, RV outflow tract and LV free wall pacing. Data presented as mean±SD, all significance $p < 0.05$ with * describing differences to RA, †RV vs. CRT modes, ‡ apical LV pacing vs. CRTa, § free wall LV pacing vs. CRTfw, ‖ CRTa vs. CRTfw, # Control vs. Esmolol or A-V Node Ablation.

Table 2. Effects of Pacing Site on Regional Left Ventricular Time to Peak Strain and Global Peak Radial Strain

Baseline Conditions (n=8)

	RA	RV	Apical LV	Free wall LV	Apical BiV	Free wall BiV
Dyssynchrony index, ms	31±15	234±60*	117±36*	145±96*	69±31*†‡	98±63*†
Standard deviation of time-to-peak strain, ms	13±5	99±28*	46±16*	43±25*	26±11*†‡	37±22*†
Global peak radial strain, %	32±10	19±11*	27±12	26±14	27±10†	24±13

During Esmolol Infusion (n=8)

	RA	RV	Apical LV	Free wall LV	Apical BiV	Free wall BiV
Dyssynchrony Index, ms	41±15	274±33*	74±46*	196±97*	76±42*†	81±39*†§
Standard deviation of time-to-peak strain, ms	16±5	117±24*	30±18*	76±38*	28±13*†	33±16*†§
Global peak radial strain, %	34±15	18±14*	26±11*	16±13*#	25±14	23±10*

Abbreviations as in **Table 1**. All data presented in mean±SD, all significance $p < 0.05$ with * describing differences to RA, ,†RV vs. BiV modes, ‡ apical LV pacing vs. apical BiV pacing, § free wall LV pacing vs. free wall BiV pacing, # Control vs. Esmolol

Figure 1. Effect of Pacing Site on Global LV Performance

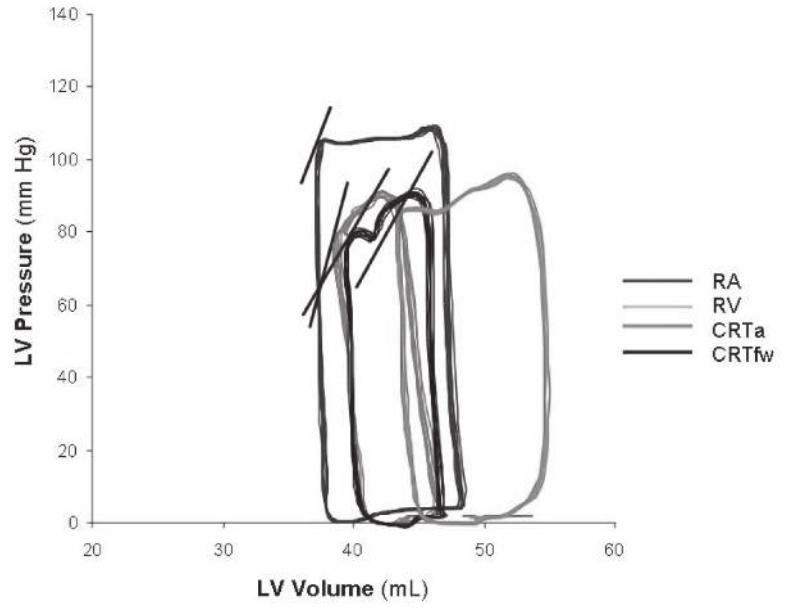

Representative apneic steady state LV pressure-volume relations during baseline RA, RV, CRTa and CTRfw with their respective end-systolic pressure-volume relations superimposed as straight lines.

Figure 2. Effect of Uni-LV and BiV Pacing on LV Pressure-Volume Relations

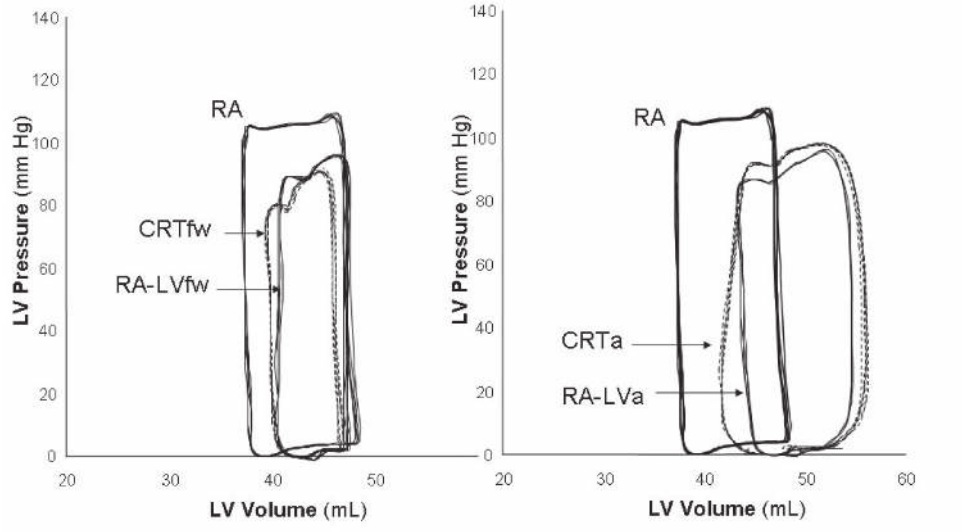

Comparison of RA-LV with RA-RV-LV (CRT) pacing on LV pressure volume relations for LV free wall (left) and apical (right) sites. Note that RA-LV pacing produces LV pressure-volume histories similar but not identical to their respective CRT pacing pairs and quite distinct from the RA pacing alone. Abbreviations as in **Figure 1**.

Figure 3. Effect of Pacing Site on Maximal Contraction Delay

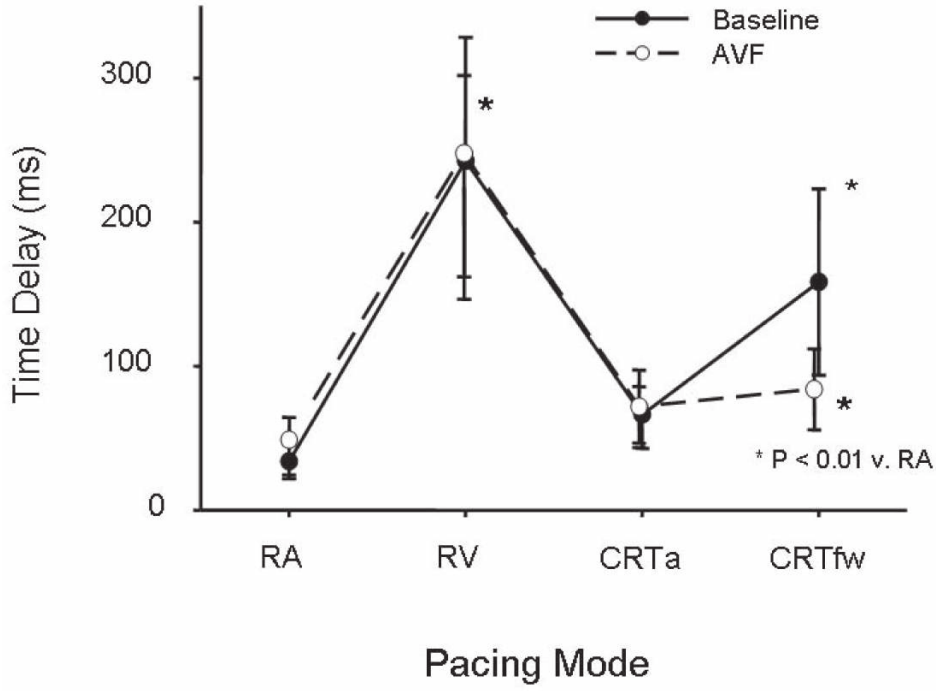

Mean±SD time to maximal strain across all regions for all animal (n=8) for RA, RA-RV, CRTa and CRTfw during baseline and esmolol-induced beta adrenergic blockade conditions. Abbreviations as in **Figure 1**

Figure 4. Relation Between Pacing-Induced Dyssynchrony Change and SW Changes

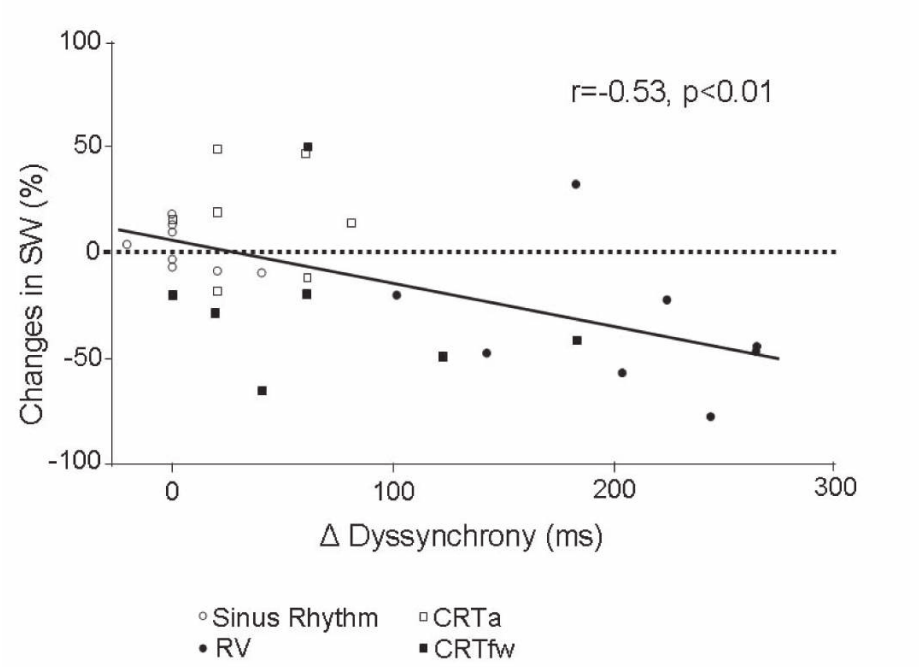

Relation between change in dyssynchrony index (Δ Dyssynchrony) and stroke work (SW) from RA pacing control. Δ Dyssynchrony is the arithmetic difference between dyssynchrony index of RA pacing versus other sites. Changes in SW were calculated as the ratio of the difference is SW between RA pacing and experimental to the RA pacing SW x 100.

Figure 5. Effect of Pacing Site and Pericardial Restraint on Global LV Function

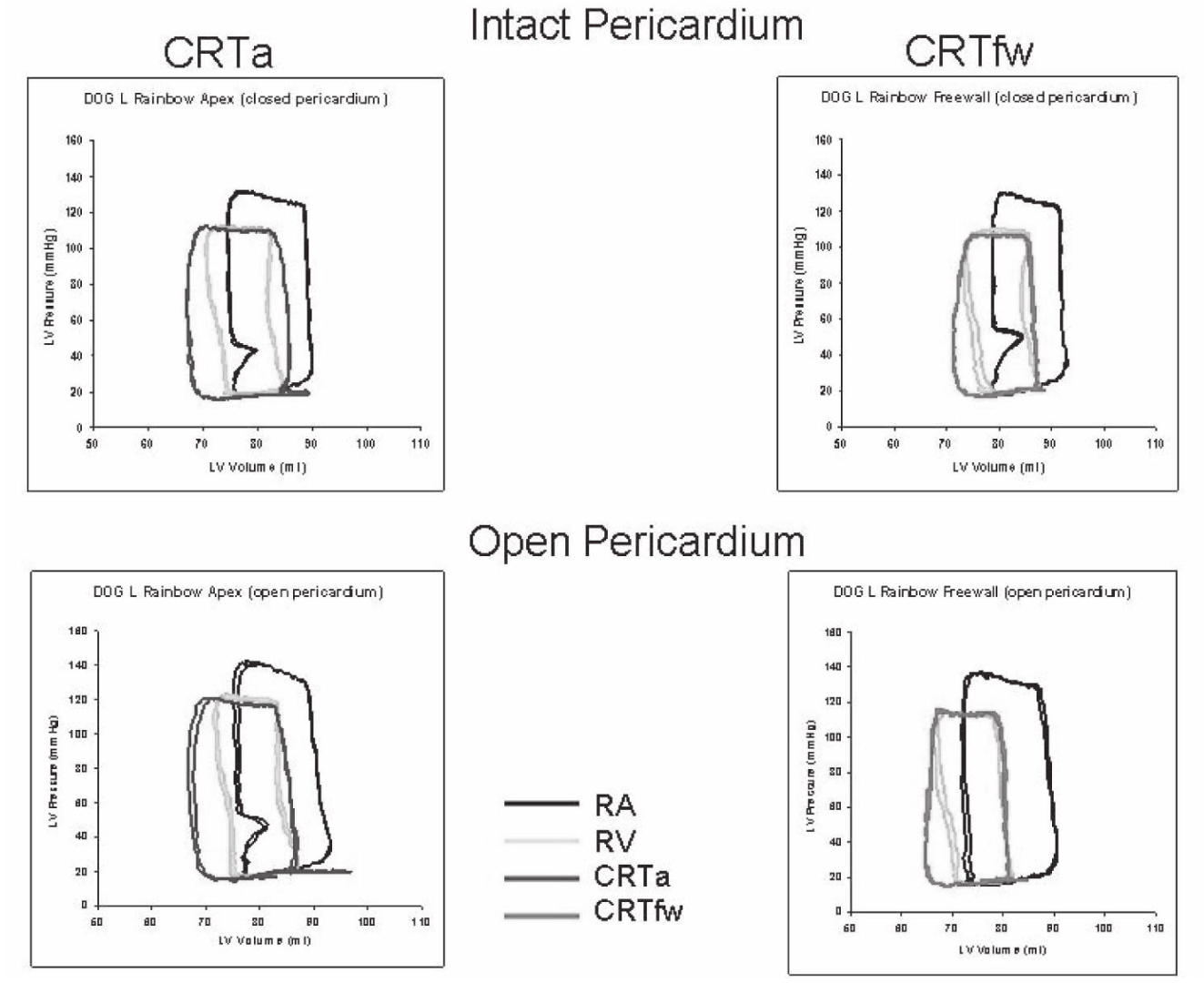

Effect of rapidly sequential pacing site progression from RA to RA-RV to CRTal (left) and CRTfw (right) and the presence (top) or absence (bottom) of an intact pericardium on the LV pressure-volume relations during baseline conditions. Each pacing site state was used for only 2-3 beats before adding additional pacing sites. Abbreviations as in **Figure 1**

Figure E1. Effect of Pacing Site on Global LV Performance

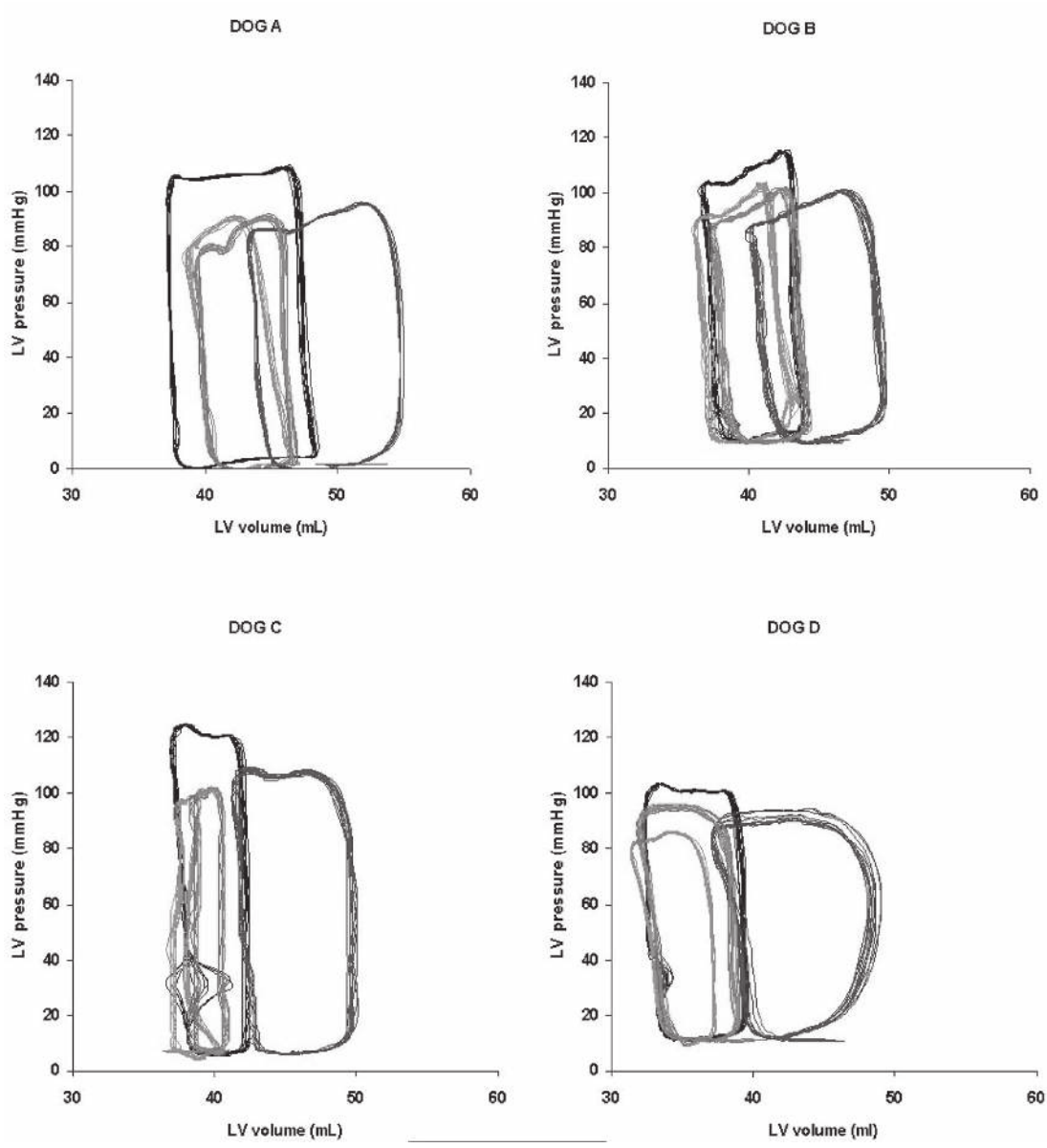

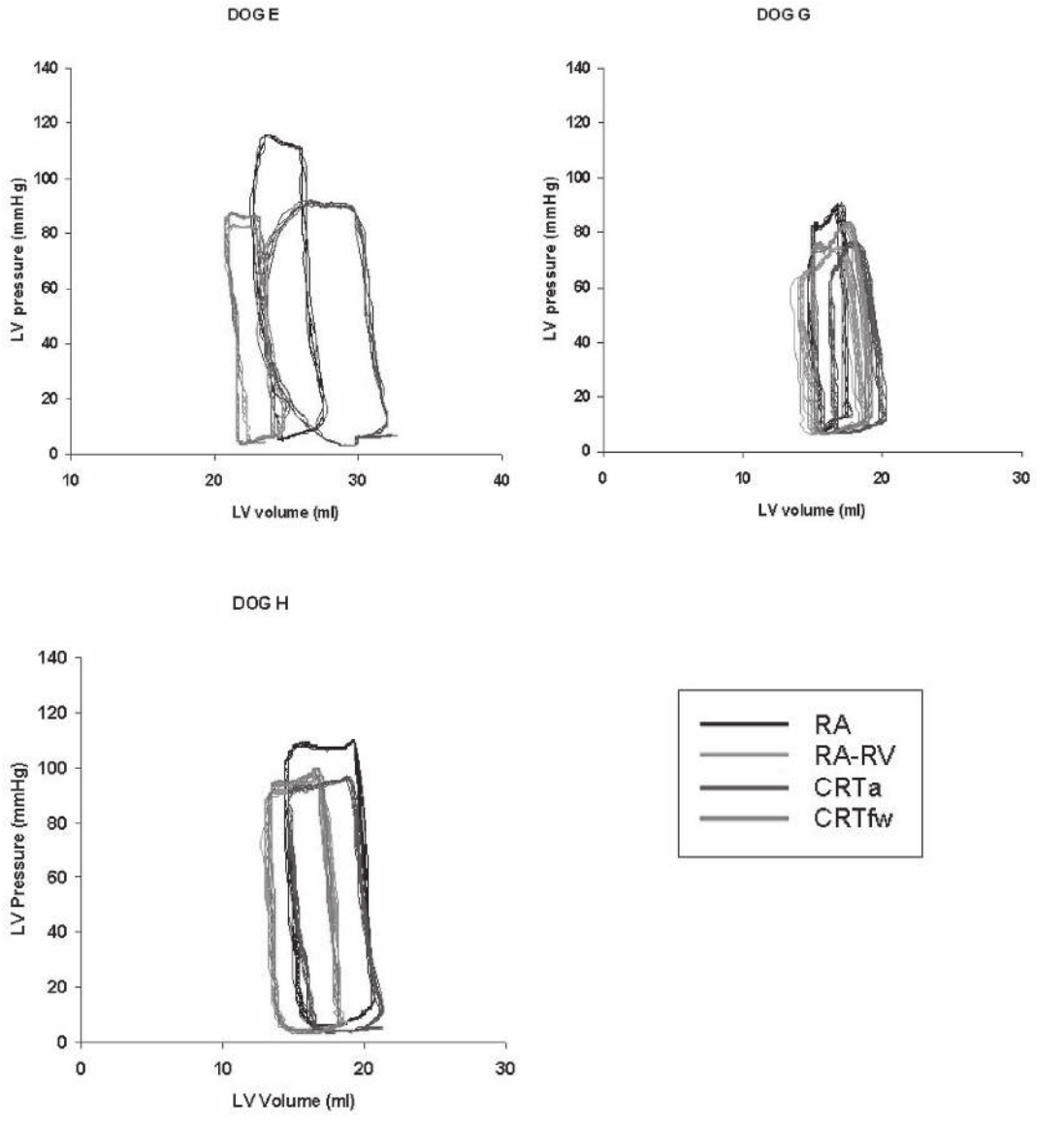

Apneic steady state left ventricular (LV) pressure-volume relations during baseline RA, RA-RV, CRTa and CRTfw with their respective end-systolic pressure-volume relations superimposed as straight lines for all animals except the one shown in **Figure 1**.

References

1. Kass DA, Chen CH, Curry C, Talbot M, Berger R, Fetics B, et al. Improved LV mechanics from acute VDD pacing in patients with dilated cardiomyopathy and ventricular conduction delay. Circulation 1999;99:1567-73.
2. Cazeau S, Leclercq C, Lavergne T, Walker S, Varma C, Linde C, et al. Effects of multisite biventricular pacing in patients with heart failure and intraventricular conduction delay. N Engl J Med 2001;344:873-80.
3. Bristow MR, Saxon LA, Boehmer J, Krueger S, Kass DA, DeMarco T, et al. Cardiac-resynchronization therapy with or without an implantable defibrillator in advanced chronic heart failure. N Engl J Med 2004;350:2140-50.
4. Breithardt OA, Stellbrink C, Kramer AP, Sinha AM, Franke A, Salo R, et al. Echocardiographic quantification of left ventricular asynchrony predicts an acute hemodynamic benefit of cardiac resynchronization therapy. J Am Coll Cardiol 2002;40:536-45.
5. Bleeker GB, Mollema SA, Holman ER, Van de Veire N, Ypenburg C, Boersma E, et al. Left ventricular resynchronization is mandatory for response to cardiac resynchronization therapy: analysis in patients with echocardiographic evidence of left ventricular dyssynchrony at baseline. Circulation 2007;116:1440-8.
6. Bleasdale RA, Turner MS, Mumford CE, Steendijk P, Paul V, Tyberg JV, et al. Left ventricular pacing minimizes diastolic ventricular interaction, allowing improved preload-dependent systolic performance. Circulation 2004;110:2395-400.
7. Dohi K, Pinsky MR, Kanzaki H, Severyn D, Gorcsan J 3rd. Effects of radial left ventricular dyssynchrony on cardiac performance using quantitative tissue Doppler radial strain imaging. J Am Soc Echocardiogr 2006;19:475-82.
8. Johnson L, Kim HK, Tanabe M, Gorcsan J, Schwartzman D, Shroff SG, et al. Differential effects of left ventricular pacing sites in an acute canine model of contraction dyssynchrony. Am J Physiol Heart Circ Physiol 2007;293:H3046-55.
9. Pinsky MR, Rico P. Cardiac contractility is not depressed in early canine endotoxic shock. Am J Respir Crit Care Med 2000;161:1087-93.
10. Dohi K, Suffoletto MS, Schwartzman D, Ganz L, Pinsky MR, Gorcsan J 3rd. Utility of echocardiographic radial strain imaging to quantify left ventricular dyssynchrony and predict acute response to cardiac resynchronization therapy. Am J Cardiol 2005;96:112-6.
11. Gorcsan J 3rd, Denault A, Mandarino WA, Pinsky MR. Left ventricular pressure-volume relations with transesophageal echocardiographic automated border detection: comparison with conductance-catheter technique. Am Heart J 1996;131:544-52.
12. Sade LE, Severyn DA, Kanzaki H, Dohi K, Gorcsan J 3rd. Second-generation tissue Doppler with angle-corrected color-coded wall displacement for quantitative assessment of regional left ventricular function. Am J Cardiol 2003;92:554-60.
13. Sade LE, Kanzaki H, Severyn D, Dohi K, Gorcsan J 3rd. Quantification of radial mechanical dyssynchrony in patients with left bundle branch block and idiopathic dilated cardiomyopathy without conduction delay by tissue displacement imaging. Am J Cardiol 2004;94:514-8.
14. Strum DP, Pinsky MR. Modeling of asynchronous myocardial contraction by effective stroke volume analysis. Anesth Analg 2000;90:243-51.
15. Peschar M, de Swart H, Michels KJ, Reneman RS, Prinzen FW. Left ventricular septal and apex pacing for optimal pump function in canine hearts. J Am Coll Cardiol 2003;41:1218-26.
16. Bordachar P, Lafitte S, Reuter S, Garrigue S, Sanders P, Roudaut R, et al. Biventricular pacing and left ventricular pacing in heart failure: similar hemodynamic improvement despite marked electromechanical differences. J Cardiovasc Electrophysiol 2004;15:1342-7.
17. Helm RH, Byrne M, Helm PA, Daya SK, Osman NF, Tunin R, et al. Three-dimensional mapping of optimal left ventricular pacing site for cardiac resynchronization. Circulation 2007;115: 953-61.
18. Frias PA, Corvera JS, Schmarkey L, Strieper M, Campbell RM, Vinten-Johansen J. Evaluation of myocardial performance with conventional single-site ventricular pacing and biventricular pacing in a canine model of atrioventricular block. J Cardiovasc Electrophysiol 2003;14:996-1000.
19. Wyman BT, Hunter WC, Prinzen FW, Faris OP, McVeigh ER. Effects of single- and biventricular pacing on temporal and spatial dynamics of ventricular contraction. Am J Physiol Heart Circ Physiol 2002;282:H372-9.
20. Prinzen FW, Van Oosterhout MF, Vanagt WY, Storm C, Reneman RS. Optimization of ventricular function by improving the activation sequence during ventricular pacing. Pacing Clin Electrophysiol 1998;21:2256-60.
21. Vanderheyden M, De Backer T, Rivero-Ayerza M, Geelen P, Bartunek J, Verstreken S, et al. Tailored echocardiographic interventricular delay programming further optimizes left ventricular performance after cardiac resynchronization therapy. Heart Rhythm 2005;2:1066-72.
22. Dekker AL, Phelps B, Dijkman B, van der Nagel T, van der Veen FH, Geskes GG, et al. Epicardial left ventricular lead placement for cardiac resynchronization therapy: optimal pace site selection with pressure-volume loops. J Thorac Cardiovasc Surg 2004;127:1641-7.
23. Grines CL, Bashore TM, Boudoulas H, Olson S, Shafer P, Wooley CF. Functional abnormalities in isolated left bundle branch block. The effect of interventricular asynchrony. Circulation 1989;79:845-53.
24. Ingles Jr NB, Daughters GT, Nikolic SD, DeAnda A, Moon MR, Bolger AF, et al. Left ventricular diastolic suction with zero left atrial pressure in open-chest dogs. Am J Physiol Heart Circ Physiol 1996;270:H1217-24.
25. Grover M, Glanz SA. Endocardial pacing site affects left ventricular end-diastolic volume and performance in the intact anesthetized dog. Circ Res 1983;53:72-85.
26. Kang SJ, Song JK, Yang HS, Song JM, Kang DH, Rhee KS, et al. Systolic and diastolic regional myocardial motion of pacing-induced versus idiopathic left bundle branch block with and without left ventricular dysfunction. Am J Cardiol 2004;93:1243-6.
27. Arisi G, Macchi E, Corradi C, Lux RL, Taccardi B. Epicardial excitation during ventricular pacing. Relative independence of breakthrough sites from excitation sequence in canine right ventricle. Circ Res 1992;71:840-9.
28. Takata M, Harasawa Y, Beloucif S, Robotham JL. Coupled vs. uncoupled pericardial constraint: effects on cardiac chamber interactions. J Appl Physiol 1997;83:1799-813.
29. Schertz C, Pinsky MR. Effect of the pericardium on systolic ventricular interdependence in the dog. J Crit Care 1993;8:17-23.